Journal of Chromatography, 631 (1993) 115–124
Elsevier Science Publishers B.V., Amsterdam

CHROMSYMP. 2625

High-performance liquid chromatography of amino acids, peptides and proteins

CXXIV☆. Physical characterisation of fluidized-bed behaviour of chromatographic packing materials

Gopal Dasari, Ian Prince and Milton T. W. Hearn

Centre for Bioprocess Technology, Monash University, Clayton, Victoria - 3168 (Australia)

ABSTRACT

Bed expansion characteristics of several different chromatographic sorbent materials have been studied in liquid–solid fluidized bed systems with different column diameters. The sorbents used were sized below particle diameters (d_p) of 100 μm, and most were non-spherical in shape. The effect of particle shape and size distribution on the bed expansion behaviour and the values of bed expansion index were evaluated in relation to existing empirical correlations of bed voidage and fluid velocity under laminar flow conditions. The effect of fluid properties on the bed behaviour was studied using viscous bovine amniotic fluid as the feed stock. An axial dispersion model was used to compare the liquid mixing behaviour of the fluidized bed system with two different particle sizes of porous silica in 2.24 cm I.D. and 5.0 cm I.D. columns. The results on the bed expansion characteristics with these systems are discussed in terms of the dispersion coefficient, D_x and the Peclet number N_{pe}, for these sorbents fluidised under laminar flow conditions.

INTRODUCTION

Since the late 1940s, liquid–solid fluidized beds have been widely used in many areas of the chemical industry, for example, in ion-exchange adsorption in wastewater management and hydrometallurgical operations. Extension of these techniques to biotechnological applications in the 1960s and 1970s met with limited success, partly due to the limitations with physical parameters, such as the small density differences between the liquid feedstock and the solid particle, but also due to the complexity of the feed stock composition. In recent years, however, there has been renewed interest in the applications of fluidized bed systems in biotechnological applications with the emergence of improved sorbents capable of exhibiting the desired physical and adsorptive characteristics.

Packed bed systems are the most commonly used configuration for the chromatographic separation of proteins. On a large scale, packed bed systems often pose considerable operational difficulties when large volumes of viscous fluids are involved. In addition, most feedstocks require clarification and removal of particulate matter (cell debris, etc.) to avoid clogging of the packed bed. Moreover, with industrial process bed systems, packed with the more widely used type of soft, deformable, adsorbent particles, flow-rates must be tighty constrained to avoid high operating pressures and concomitant bed compression. The application of fluidized bed systems conceptually thus offers a number of advantages over packed bed chromatographic columns for large-scale operation, particularly when large vol-

Correspondence to: Milton T. W. Hearn, Centre for Bioprocess Technology, Monash University, Clayton, Victoria 3168, Australia.

☆ For Part CXXIII see ref. 38.

0021-9673/93/$06.00

umes of fluid must be treated to isolate and purify a bioproduct which may be present in only very low concentrations.

Included in these potential advantages are: (i) High flow-rates are possible at comparatively low operational pressures. Low pressure drop operations allow much easier process scale-up and eliminate the need for high pressure pumping equipment. (ii) Pretreatment or removal of particulate/cellular matter from fermentation broths or biological fluids may not be necessary prior to adsorption. Since the adsorbent particles in the fluidized bed are separated from each other by upward (or downward) flow of the liquid, the broth solids may be able to pass through the bed without clogging. When used in this way, fluidized beds potentially eliminate the costly removal of solids by centrifugation or filtration (see for example refs. 1–8). (iii) Greater flexibilty exists for continuous modes of operation under automated and semi-automated conditions. It is conceivable that after the initial adsorption stage is completed, the adsorbent material from the fluidized bed could be pumped out by increasing the fluid velocity, to a second fluidized column, where the washing of adsorbent can be carried out, and then pumped to a third column where the desorption of protein can be carried out.

Counter-balancing these advantages are potential problems whose magnitude remains unknown [1,4] but include the potential for reduced bed capacity, unfavourable mixing at some liquid flow-rates, particle size segregation and adventitious particulate loading.

Preliminary studies on fluidized beds in this and other laboratories [2,3,5,7–9] have demonstrated the feasibility of the technique for the fractionation of proteins and other biotechnological products. Except for one study where a magnetically stabilized fluidized bed was used [2], systems previously studied have typically employed low density, soft gels (*i.e.*, densities not dissimilar to those of the fluidizing liquid), and relatively large particles (>100 μm) with wide size distribution. Nevertheless, the substantial economic advantage that may accrue in large-scale operation has been demonstrated recently with therapeutic proteins [10] as well as with the whole broth extraction of the antibiotic immunomycin [6]. With the advent of high density adsorbent particles, specifically developed in narrow size ranges for fluidized applications, and their further refinement and surface modification in these laboratories [11] and elsewhere (see for example ref. 12), the performance characteristics of fluidization systems in biotechnological application are likely to be further enhanced in the near future.

The bed expansion characteristics of liquid–solid fluidized bed systems in various traditional chemical applications have been studied by many investigators [13–21]. Almost invariably large particles ($d_p > 100$ μm) have been used. Various applications of these large particle systems have been reviewed by Joshi [22]. Many correlations have been proposed from these investigations to establish a velocity–voidage relationship for fluidization and sedimentation with these liquid–solid systems. The majority of these correlations are applicable over a restricted range of Reynolds numbers. Among all, the correlation of Richardson and Zaki [16] has received particularly widespread recognition and use. For fluidized beds of homogeneous rigid spherical particles, these authors have proposed that the relationship between the liquid superficial velocity U, and the terminal settling velocity in infinite medium, U_i, can be given by

$$\frac{U}{U_i} = \varepsilon^n \tag{1}$$

where

$$\log U_i = \log U_t - \frac{d_p}{D} \tag{2}$$

and U_t is the particle terminal settling velocity, ε is the bed voidage, d_p is the particle diameter, and D is the column diameter.

The bed expansion index, n, is a function of the terminal settling Reynolds number (N_{Ret}) and the particle to bed diameter ratio, (d_p/D), such that over the range $0.2 < N_{Ret} < 500$ the value of n can be approximated by:

$n = 4.65 + 20\ (d_p/D)$	$(N_{Ret} < 0.2)$
$n = 4.4 + 18\ (d_p/D)\ N_{Ret}^{-0.03}$	$(0.2 < N_{Ret} < 1)$
$n = 4.4 + 18\ (d_p/D)\ N_{Ret}^{-0.1}$	$(1 < N_{Ret} < 200)$
$n = 4.4\ N_{Ret}^{-0.1}$	$(200 < N_{Ret} < 500)$
$n = 2.4$	$(N_{Ret} > 500)$

For spherical particles greater than 100 μm in average diameter, fluidized in large diameter tubes,

the values of n range between 2.39 for large N_{Ret} values and 4.65 for $N_{Ret} < 0.2$. Recently, Rowe [23] developed a logistic curve for the above correlation and related n and N_{Ret}, for cases where the particle size is small compared to column diameter, as a continuous function encompassing laminar through to turbulent flow regimes. However, with small ($d_p < 100$ μm) spherical [24] and non-spherical particles [18], larger values of n have been obtained compared to the values predicted by eqn. 2. In particular, the study of Jottrand [18] has shown that for finely crushed sands, with particle sizes ranging from 20 to 113 μm, fluidized in water, a constant value of $n = 5.6$ was observed in the laminar flow range, $0.004 < N_{Ret} < 0.7$, which is substantially lower than the range investigated by Richardson and Zaki [16].

Fouda and Capes [21] have proposed a modified form of the Richardson and Zaki [16] correlation, namely

$$\frac{U}{U_t} = [1 - k\ (1 - \varepsilon)]^n \quad (3)$$

to account for non-spherical shapes of the particles, with similar relations between n and N_{Ret} applying for spherical particles. The parameter k was introduced to account for the effective hydrodynamic volume of the particles during fluidization.

Data on axial dispersion effects in fluidized beds are scarce, with only a limited number of studies [25–31] having been performed with spherical particles above 100 μm in average particle diameter. No general correlation for axial dispersion coefficients in liquid–solid fluidized beds, which incorporates the effects of liquid velocity, particle size and column diameter, is currently available. However, Gunn [28] has discussed the results of Kramers *et al.* [25], Bruinzeel *et al.* [26], and Cairns and Prausnitz [27] in terms of the Peclet number ($N_{Pe} = UL/D_x$) and the Reynolds number ($N_{Re} = d_p U\rho/\mu$) for the purpose of comparison (where L = axial distance of fluidized bed, ρ = fluid density and μ = fluid viscosity). The effect of the ratio of the column to particle diameter encompassing the range $17 < (D/d_p) < 50$ on liquid mixing has been documented in the results of two studies [25,27] whilst the results of Bruinzeel *et al.* [26] indicate that there was no effect of the D/d_p ratio on liquid mixing over the range, $500 < (D/d_p) < 5000$. No general correlation between Peclet number and the Reynolds number has emerged from these three studies. Chung and Wen [29] studied the axial liquid mixing in fluidized and fixed beds using sinusoidal and pulse response techniques with a fluorescein dye as a tracer. A systematic study of fluidization of glass, aluminium and steel particles (d_p in the range 0.20–0.64 cm) in water in a 5.08-cm I.D. column was carried out by these investigators. For the Reynolds number ranging from 51 to 1286, they obtained values of Peclet numbers in the range of 0.1 to 0.91. Moreover, these investigators found that the dispersion coefficient increased with increases in liquid velocity for constant particle density. From these experimental data and other data from the literature, a correlation of liquid axial dispersion coefficients of fixed and fluidized beds in terms of Peclet number and Reynolds number was developed by Chung and Wen [29]. Recently, Webster and Perona [30,31] have studied the liquid mixing characteristics in cylindrical and tapered liquid–solid fluidized beds with three particle sizes of glass (average d_p 114, 440 and 1210 μm) and 320 μm size coal particles. Their results show that the dispersion coefficient decreased for 114 μm size glass and for 320 μm size coal particles but increased for bigger size particles of glass with increasing void fraction or liquid velocity in a cylindrical column. However, they found that the Peclet number also increased Reynolds numbers.

The rehological characteristics of biological fluids can be anticipated to have considerable bearing on the design and the operation of a fluidized bed system for protein recovery and purification processes. An increase in fluid viscosity would decrease the range of liquid velocities achievable in the fluidized bed, since the terminal settling velocity of particles is inversely related to the viscosity of the fluid. In addition, the fluid characteristics play an important role in the mixing behaviour, and mass transfer. These effects will impact on the detector or biosensor responses required for the on-line control monitoring of the bioprocessing of crude feedstocks during scale-up procedures [32].

In order for the full potential of fluidized systems to be evaluated for biorecovery and biopurification tasks, fundamental characterisation of these systems must be achieved. This study examines the fluidized bed characteristics, in terms of bed expansion and liquid mixing as a function of liquid superficial velocity, with various sizes of chromatographic sor-

bent materials of spherical and non-spherical particles suspended in columns of different internal diameters. The effect of liquid properties on bed expansion behaviour was also studied using bovine amniotic fluid.

EXPERIMENTAL

Materials

Lichroprep Si 60 (average pore size 6 nm) silica in two types of particle size range, 25–40 μm and 40–63 μm; Lichroprep-diol (average pore size 6 nm), derivatised silica 40–63 μm; Fractosil 1000 (average pore size 100 nm) silica 63–100 μm and Fractogel TSK HW55(F) (pores could accommodate up to 90 000 molecular mass proteins), 32–63 μm were obtained from E. Merck (Darmstadt, Germany). Fluorescein (water soluble) tracer was obtained from Selbys (Melbourne, Australia). Bovine amniotic fluid was supplied by Filtron (Melbourne, Australia).

Methods

Particle size analysis for all the sorbent samples was performed using a Malvern 2600 particle sizer. The Sauter mean diameter (S.M.D.) was computed based on the size distribution by weight percent in each size range.

Viscosity measurements were performed using a Contraves Low Shear 30 sinus rheometer with temperature control arrangement. This rheometer is capable of measuring the rheological properties of low viscosity fluids in both the steady and oscillatory modes yielding data such as shear stress, storage modulus and loss modulus. The shear rate ranges from 0.02 to 118.2 s^{-1}, with different bob and cup geometry, with 1–3 ml sample holding capacity. The viscosity of bovine amniotic fluid was measured at 20°C.

Particle density of porous silica gels and Fractogel in water were measured by the displacement method. A known amount of gel was soaked in water and degassed, then the gel was filtered using vacuum suction pump at 3333 Pa to remove the interstitial water. A known amount (25 g) of this gel was placed in a measuring cylinder and the total volume was measured by adding 20 ml of water to the gel. The displaced volume is equivalent to the volume of the gel. The particle density calculation was based on the known weight and the volume of the gel. The density of amniotic fluid was measured using a specific gravity bottle at 20°C.

Fluidized bed studies

Fig. 1 is a schematic diagram showing the experimental set-up used in the bed expansion characteristics and residence time distribution (RTD) studies. Two columns of 100 cm^3 (2.24 cm I.D. × 26 cm) and 200 cm^3 (2.34 cm I.D. × 54 cm) volume, made of polycarbonate material, and one column of 1000 cm^3 (5 cm I.D. × 60 cm) volume, made of glass using an adapted Pharmacia K 50 column (Pharmacia Aust., Sydney, Australia), were used in these studies. All these columns had a bottom distributor section, filled with glass beads (d_p 250 μm), to permit uniform distribution of the liquid into the column. The adjustable adaptors at the top on the columns were fitted with 10 μm nylon filters to prevent the loss of sorbent particles. Except where bovine amniotic fluid was used, all other studies were performed with distilled water as a liquid medium at 22°C.

Measurement of degree of mixing or dispersion

The degree of mixing or dispersion in a fluidized bed was determined using residence time distribu-

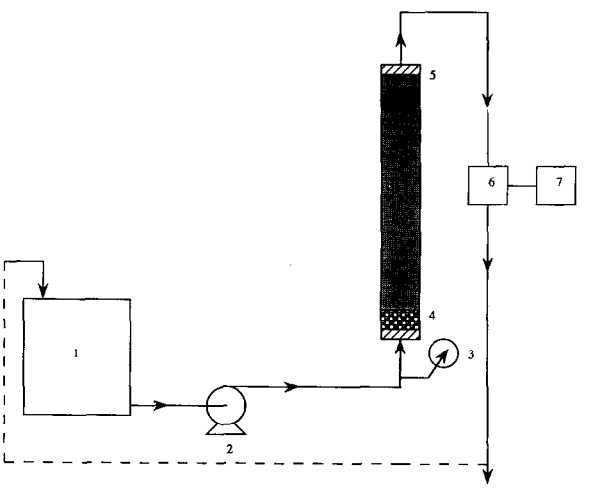

Fig. 1. Schematic diagram of a fluidized bed set up: 1 = feed tank, 2 = pump, 3 = pressure gauge, 4 = distributor, 5 = adjustable adaptor with retension filter, 6 = spectrophotometer with flow cell arrangement, 7 = chart recorder.

tion (RTD) studies. The pulse injection technique has been used, employing fluorescein as a tracer. To achieve a good tracer pulse injection, a micro-syringe was used to inject 100 μl of fluorescein (5 mg/ml) under stable bed conditions. The adaptors at the top of fluidized columns were adjusted close to the expanded bed upper surface to avoid dead space effects in the columns. The effluent was recorded continuously at a wavelength of 490 nm using a spectrophotometer (LKB, Ultrospec-II) with flow cell arrangement. These studies were performed in two different column diameters with various amounts of porous silica gel (Lichroprep Si 60) with two particle size ranges.

The axial dispersion model [33] was used to estimate the degree of liquid dispersion in the fluidized bed system. The extent of mixing was measured by calculating the dispersion number (D_x/UL) from the data of the tracer response curves. The axial dispersion number estimation was based on the closed vessel situation since the techniques used for injection and dispersion sampling represent the closed vessel boundary conditions.

RESULTS AND DISCUSSION

Bed expansion characteristics

The ration of height of the expanded bed to the settled bed (H_L/H_0) with increasing liquid velocities (U) for all the studied sorbent materials and the columns of different diameters is plotted in Fig. 2. The results evident from these (H_LH_0) *versus* U plots clearly indicate that the operating range of liquid velocities for the Fractogel TSK HW55F is very narrow due to its low particle density. On the other hand, the velocity range for Fractosil 1000 material is rather broad, due to its higher particle density and larger particle size range compared to Fractogel TSK HW55F or other sorbents. The bed expansion results for Lichroprep Si 60 in two particle size distributions show the effect of particle size on the operating range of liquid velocities that can

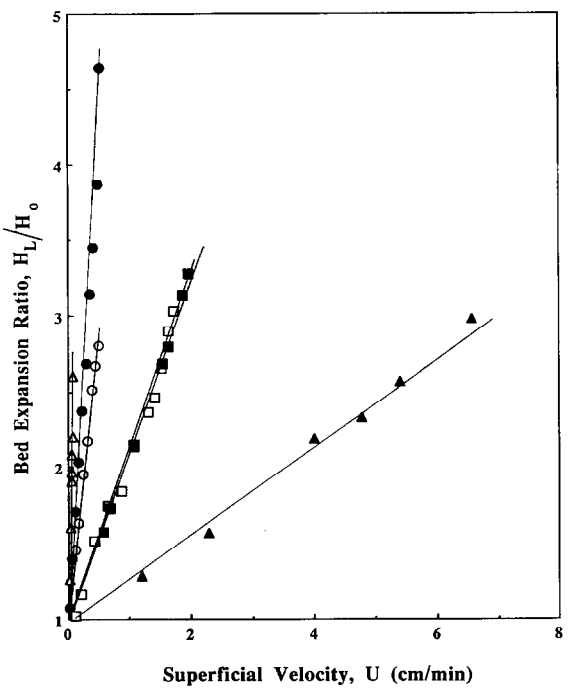

Fig. 2. Fluidized bed expansion characteristics in columns with varying diameters using different chromatographic materials. (○) 25–40 μm, Lichroprep Si 60, 2.24 cm I.D.; (□) 40–63 μm Lichroprep Si 60, 2.24 cm I.D.; (●) 25–40 μm, Lichroprep Si 60, 5.00 cm I.D.; (■) 40–63 μm, Lichroprep Si 60, 5.00 cm I.D.; (△) 32–63 μm, Fractogel TSK HW 55F, 2.34 cm I.D.; (▲) 63–100 μm, Fractosil 1000, 2.34 cm I.D.

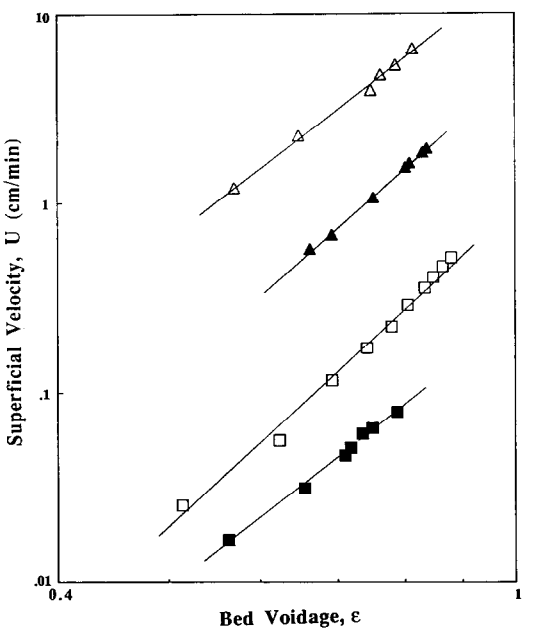

Fig. 3. Liquid superficial velocity *versus* bed voidage for different chromatographic materials. (□) Lichroprep Si 60, 25–40 μm; (▲) Lichroprep Si, 40–63 μm; (■) Fractogel TSK HW 55F, 32–63 μm; (△) Fractosil 1000, 63–100 μm.

TABLE I

PHYSICAL PROPERTIES AND BED EXPANSION CHARACTERISTICS OF PARTICLES

	Particle size range (μm)	Mean diameter (μm)	Shape	Shape factor (Φ)	Particle density (g/cm^3)	N_{Ret}	Bed expansion index (n)
Richardson and Zaki [16]	[a]	>100	Spherical	1.00	[a]	<0.2	4.65
Jottrand [18]	[a]	20.2	Angular (crushed sand)	0.73	2.685	0.004[b]	5.60
		28.7	Angular (crushed sand)	0.73	2.685	0.012	5.60
		43.1	Angular (crushed sand)	0.73	2.685	0.039	5.60
		63.0	Angular (crushed sand)	0.73	2.685	0.111	5.60
		86.2	Angular (crushed sand)	0.73	2.685	0.312	5.60
		113.0	Angular (crushed sand)	0.73	2.685	0.706	5.60
LiChroprep Si 60	24–50	24.9	Angular	0.73	1.345	0.001	5.77 ± 0.56[c]
	40–63	62.9	Angular	0.73	1.361	0.019	5.27 ± 0.28[c]
LiChroprep-diol	40–63	61.9	Angular	0.73	1.311	0.016	5.02
Fractosil 1000	63–100	80.9	Angular	0.,73	1.389	0.044	4.68
Fractogel TSK HW55(F)	32–63	48.4	Spherical	1.00	1.087	0.005	4.74

[a] Not reported by these investigators.

[b] N_{Ret} values were calculated based on Jottrand's data assuming $\Phi_s = 0.73$, for the purpose of comparison.

[c] Standard deviation.

be obtained in two columns of different diameters. The results also indicate that the effect of column diameter on the bed expansion behaviour is negligible.

The bed voidage *versus* liquid velocity data for all the sorbent materials exhibited linear relationships in their log–log plots (Fig. 3). The slope of these plots yields the bed expansion index (n), whilst extrapolation of the data to $\varepsilon = 1$ yields U_t, the terminal settling velocity of the particle. The values of n are presented in Table I along with other values of n available in the literature and the physical properties of the materials used. The mean diameters of the particles used for the calculations of the present study were based on Sauter mean diameter of the particles, measured using the Malvern 2600 laser based particle sizer. The values of n varied from 5.77 to 4.68 for the angular silica gels and was 4.74 for spherical shaped Fractogel beads.

Except for Jottrand's work [18], there appear to be no other data in the literature on bed voidage–velocity relationships for small particles ($d_p < 113$ μm) of non-spherical shape (Table I). In this earlier study a single value of $n = 5.6$ was obtained for all the particle sizes of crushed sand used in liquid–solid fluidization experiments. Our results indicate that the value of n increases with the decrease in size of particles of similar shape characteristics, *e.g.* $n = 4.68$ to 5.77 for particles with average d_p ranging from 25 to 81 μm respectively. These n values correspond closely to the literature n values for larger particles. For example, the value of n reported by Richardson and Zaki [16] for spherical particles ($d_p > 100$ μm) at $N_{Ret} < 0.2$, was 4.65 based on the experimental data from sedimentation and fluidization studies with a large number of particle sizes of different densities and with liquids of various viscosities. Richardson and Meikle [24] found with sedimentation experiments involving the suspension of spheres ($d_p < 100$ μm) that N_{Ret} was less than 0.2, and the mean value of n was 4.79. These investigators also reported that for fine alumina particles (d_p 5.5 μm), the value of n was 10.5. However, Fouda and Capes [21], in studies on the effect of the particle shape factor on bed expansion characteristics, used various materials of different densities densities and particles sizes more than 137 μm in diameter except for one crushed silica with particle size of d_p 52 μm and obtained lower n values. Based on their correlation and values of k calculated for the crushed silica of d_p 52 μm, the maximum value of n was found to be only 4.49.

The larger values of n obtained in the present investigation for small particles with irregular shapes may be due to the higher levels of immobile fluid trapped with the solids due to particle agglomeriation, occlusion in surface irregularities or simply due to the increased volume of the boundary layer relative to the particle volume. This concept has been early proposed by Steinour [34–36] to account for the involvement of similar effects in the sedimentation of fine spherical, irregular and flocculated particles. This explanation may not however be valid for larger particles, as evident from our result with Fractosil 1000, where $n = 4.68$ is close to the value reported by Richardson and Zaki [16]. Their n value also fits reasonably well with our data for spherical shaped Fractogel beads (Table I).

The effect of fluid viscosity on bed expansion behaviour was studied using bovine amniotic fluid, $\mu = 1.454$ centipoise, using Lichroprep-diol porous silica (d_p 40–63 μm). The rationale behind the selection of bovine amniotic fluid for this study arose from our interest in separation and purification of pharmaceutically important growth factors from this feed-stock source [11]. Amniotic fluid comprises a complex mixture of proteins and polysaccharides. The rheological and compositional characteristics of this fluid have been determined and the results are presented in another manuscript [37]. The bed expansion results indicate a pseudoplastic behaviour. The data of shear stress and shear rate was best represented by a power law fluid. The results on these investigations are presented in Fig. 4A and B. The value of n for Lichroprep-diol silica with amniotic fluid was found to be 7.75 whilst the value with water was 5.02. The liquid properties, the values of Reynolds number based on particle terminal settling velocity and n are presented in Table II. The values of n obtained for angular silica gels indicate that there is a linear dependency on the particle size for the range of particles tested under the same fluidization conditions (Fig. 5). There also appears to be a linear relation between n and N_{Ret} for the range of Reynolds numbers studied.

Liquid mixing studies

These studies were conducted with two particle

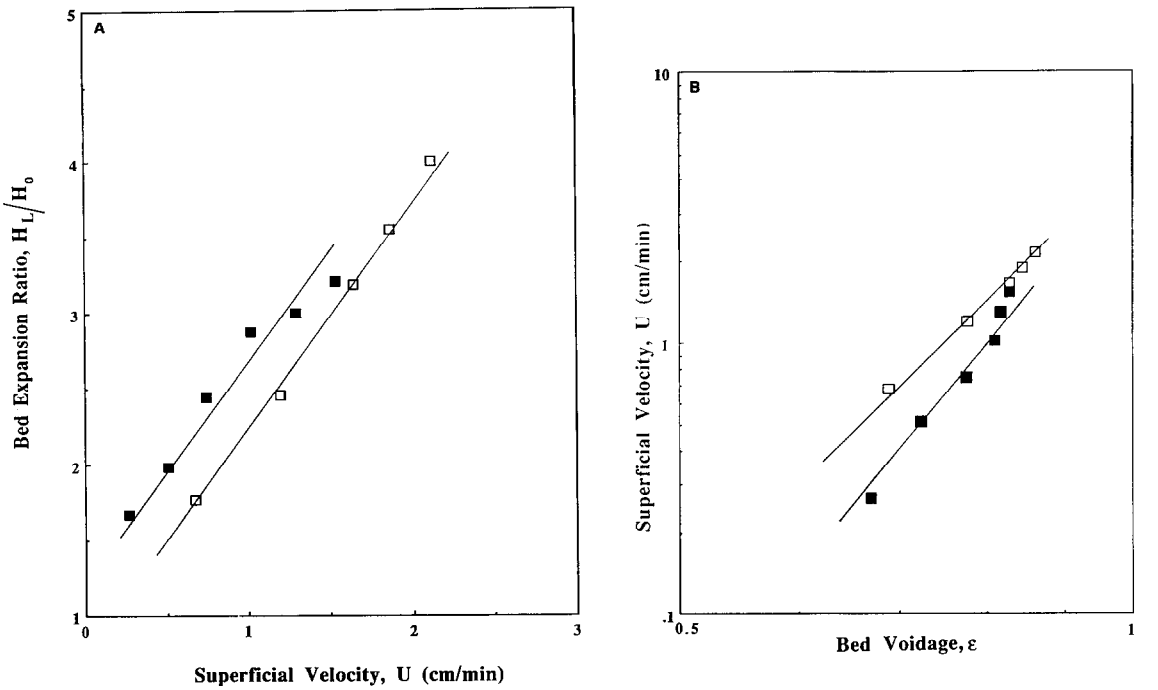

Fig. 4. (A) Effect of fluid viscosity on bed expansion characteristics: Lichroprep-diol (d_p 40–63 μm) with water and bovine amniotic fluid. (B) Effect of fluid viscosity on bed voidage: Lichroprep-diol (d_p 40–63 *v*) with water and bovine amniotic fluid. (□) Water, (■) bovine amniotic fluid.

sizes of the Lichroprep Si 60 porous silica in two fluidized columns of different diameter. The data on dispersion coefficient *versus* superficial velocity are presented in Fig. 6. These plots reveal that the dispersion coefficient increases with the increasing superficial velocity. Similar observations for large spherical particles in liquid–solid fluidization systems have been reported by Cairns and Prausnitz [27], Kramers *et al.* [25] and Chung and Wen [29]. However, Webster and Perona [30] observed that the dispersion coefficient for 114 μm size glass and 320 μm size coal particles decreased with increasing bed voidage or superficial velocity but increased for bigger size glass particles. It has also been observed in the present study with small size particles (d_p 25–40 μm) that the dispersion coefficients are higher than obtained with bigger particles in the same column system. Chung and Wen [29] noted that the effect of very large particle size (average d_p 2032–6350 μm) on dispersion coefficients with increasing velocity was not significant. As evident from our results with silica based sorbents, there is a notice-

TABLE II

EFFECT OF LIQUID PROPERTIES ON BED EXPANSION INDEX WITH LICHROPREP-DIOL SILICA GEL (40–63 μm)

Liquid	Viscosity (centipoise)	Density (g/cm^3)	N_{Ret}	Bed expansion (*n*)
Water	1.000	1.000	0.016	5.02
Bovine amniotic fluid	1.454	1.013	0.020	7.75

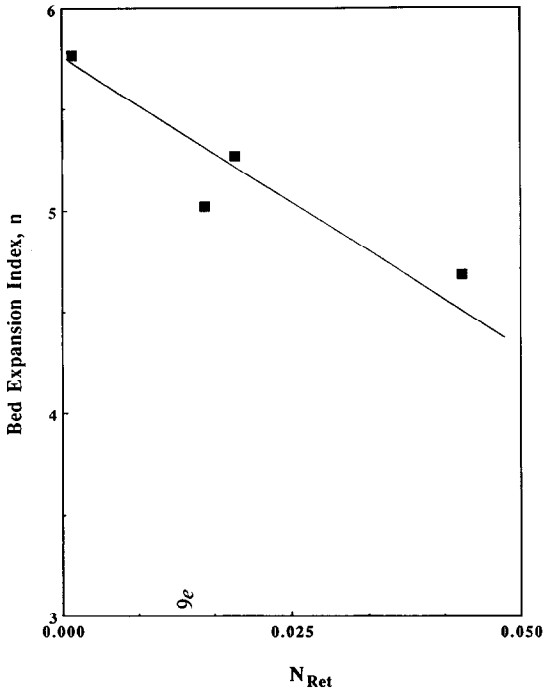

Fig. 5. Bed expansion index, *n versus* particle Reynolds number for angular silicas.

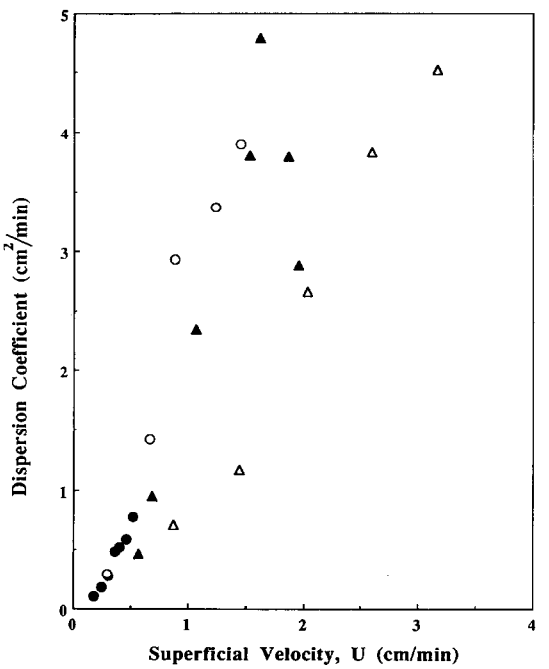

Fig. 6. Dispersion *versus* liquid velocity in fluidized beds with varying column diameter using Lichroprep Si 60 silica. (○) 25–40 μm, 5.00 cm I.D.; (●) 25–40 μm, 2.24 cm I.D.; (△) 40–63 μm, 5.00 cm I.D.; (▲) 40–63 μm, 2.24 cm I.D.

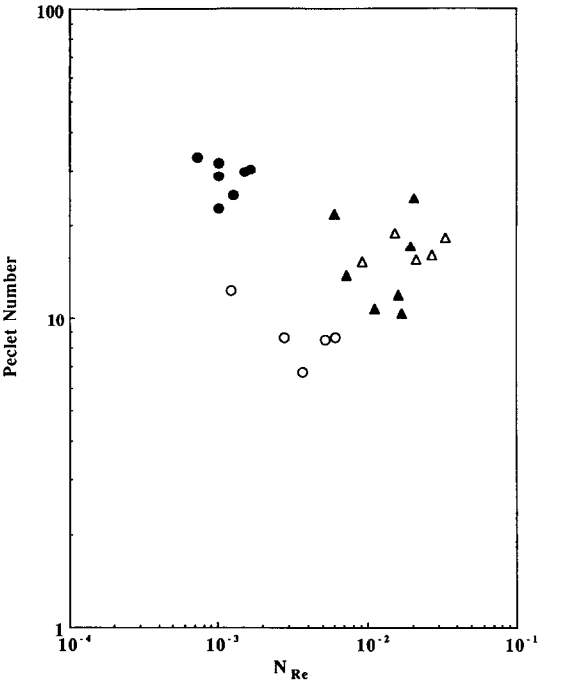

Fig. 7. Peclet number *versus* Reynolds number in fluidized beds with varying column diameter using Lichroprep Si 60 silica. (○) 25–40, 2.24 cm I.D.; (●) 40–63 μm, 2.24 cm I.D.; (△) 25–40 μm, 5.00 cm I.D.; (▲) 40–63 μm, 5.00 cm I.D.

able effect of the (D/d_p) ratio on dispersion coefficient with increasing velocities or bed voidage. The mixing data has also been evaluated in terms of Peclet number and Reynolds number based on the fluid velocity for both particle sizes. These results indicate that for the range of Reynolds numbers tested in the present study the mixing behaviour is in the regime of dispersed-plug flow. Although liquid mixing appears to be higher for small particles compared to larger particles in the 2.24 cm I.D. column, the difference in the 5 cm I.D. column is not significant (Fig. 7).

CONCLUSIONS

The bed expansion characteristics have been studied for several microparticulate angular silicas, and spherical particles of Fractogel, in terms of bed expansion and bed voidage as a function liquid superficial velocity. The higher values of bed expansion index (n) obtained for the smaller silicas could

be due to the irregular shape of the particles. The bed expansion index was found to be linearly related to the particle Reynolds number over the range tested. The liquid mixing studies performed in 2.24 and 5 cm I.D. columns with two particle sizes (d_p 25–40 and 40–63 μm) of silica exhibited dispersed-plug flow characteristics under laminar flow conditions. In associated publications, the use of these parameters in the design and application of expanded bed systems with silica-based affinity sorbents for the large scale fractionation of proteins from natural and recombinant DNA feedstock sources will be described.

ACKNOWLEDGEMENTS

These investigations were supported by the Industrial Research and Development Board, Australian Department of Industry, Trade and Commerce, and Monash University Research Fund.

REFERENCES

1 A. Buijs and J. A. Wesselingh, *J. Chromatogr.*, 201 (1980) 319.
2 M. A. Burns and D. J. Graves, *Biotechnol. Prog.*, 1 (1985) 95.
3 C. M. Wells, A. Lyddiatt and K. Patel, in M. S. Verral and M. J. Hudson (Editors), *Separation for Biotechnology*, Ellis Horwood, Chichester, 1987, pp. 217–224.
4 C. H. Lochmuller, C. S. Ronsick and L. S. Wigman, *Prep. Chromatogr.*, 1 (1988) 93.
5 W. Somers, K. van 't Reit, H. Rozie, F. M. Rombouts and J. Visser, *Chem. Eng. J.*, 40 (1989) B47.
6 F. P. Gailliot, C. Gleason, J. J. Wilson and J. Zwarick, *Biotechnol. Prog.*, 6 (1990) 370.
7 N. Drager and H. Chase, *Inst. Chem. Eng. Symp. Ser.*, 118 (1990) 161.
8 H. Chase and N. Drager, *J. Chromatogr.*, 597 (1992) 129.
9 G. Dasari, G. Finette, I. Prince and M. T. W. Hearn, *Aust. J. Biotechnol.*, 10 (1992) 312.
10 M. T. W. Hearn, G. Dasari, I. Prince, M. Bjorklund and G. Finette, *Patents Pendings* (1991).
11 M. T. W. Hearn, M. Gani, P. Chen and P. Rossiter, Patents Pending (1992).
12 K. K. Unger, in K. K. Unger (Editor), *Packings and Stationary Phases in Chromatographic Techniques*, Marcel Dekker, New York, 1990.
13 R. H. Wilhelm and M. Kwauk, *Chem. Eng. Prog.*, 44 (1948) 201.
14 W. K. Lewis, E. R. Gilliland and W. Bauer, *Ind. Eng. Chem.*, 41 (1949) 1104.
15 W. K. Lewis and E. W. Bowerman, *Chem. Eng. Prog.*, 48 (1952) 603.
16 J. F. Richardson and W. N. Zaki, *Trans. Inst. Chem. Eng.*, 32 (1954) 35.
17 A. L. Loeffler and B. F. Ruth, *AIChE J.*, 5 (1959) 310.
18 R. Jottrand, *J. Appl. Chem. (London)*, 2 Suppl. Issue I, (1952) S17-S26.
19 C. Y. Wen and Y. H. Yu, *Chem. Eng. Prog. Symp. Ser.*, 62 (1966) 100.
20 J. Garside and M. R. Al-Dibouni, *Ind. Eng. Chem. Process Des. Dev.*, 16 (1977) 206.
21 A. E. Fouda and C. E. Capes, *Can. J. Chem. Eng.*, 55 (1977) 386.
22 J. B. Joshi, *Chem. Eng. Res. Des.*, 61 (1983) 143.
23 P. N. Rowe, *Chem. Eng. Sci.*, 42 (1987) 2795.
24 J. F. Richardson and R. A. Meikle, *Trans. Inst. Chem. Eng.*, 39 (1961) 348.
25 H. Kramers, M. D. Westermann, J. H. de Groot and F. A. Dupont, *3rd Cong. Eur. Fed. Chem. Eng.*, Olympia, London, 1962, pp. 114–119.
26 C. Bruinzeel, G. H. Reman and E. Th. van der Laan, *3rd Cong. Eur. Fed. Chem. Eng.*, Olympia, London, 1962, pp. 120–126.
27 E. J. Cairns and J. M. Prausnitz, *AIChE J.*, 6 (1960) 400.
28 D. J. Gunn, *The Chemical Engineer*, London, CE153, 1968, p. 219.
29 S. F. Chung and C. Y. Wen, *AIChE J.*, 14 (1968) 857.
30 G. H. Webster and J. J. Perona, *AIChE Symp. Ser.*, 86 (276) (1987) 104.
31 G. H. Webster and J. J. perona, *AIChE J.*, 34 (1988) 1398.
32 M. Charles, *Adv. Biochem. Eng.*, 8 (1978) 1.
33 O. Levenspiel, *Chemical Reaction Engineering*, Wiley, New York, 2nd ed., 1972.
34 H. H. Steinour, *Ind. Eng. Chem.*, 36 (1944) 901.
35 H. H. Steinour, *Ind. Eng. Chem.*, 36 (1944) 840.
36 H. H. Steinour, *Ind. Eng. Chem.*, 36 (1944) 618.
37 G. Dasari, I. Prince and M. T. W. Hearn, in preparation.
38 A. W. Purcell, M. I. Aguilar and M. T. W. Hearn, *Anal Chem.*, (1992) in press.